Journal of Power Sources 239 (2013) 409–414

Contents lists available at SciVerse ScienceDirect

Journal of Power Sources

journal homepage: www.elsevier.com/locate/jpowsour

Influence of temperature and composition of NaOH–KOH and NaOH–LiOH electrolytes on the performance of a direct carbon fuel cell

A. Kacprzak*, R. Kobylecki, Z. Bis

Department of Energy Engineering, Faculty of Environmental Engineering and Biotechnology, Czestochowa University of Technology, ul. Brzeznicka 60a, 42-200 Czestochowa, Poland

HIGHLIGHTS

- The effect of molten hydroxide composition on direct carbon fuel cell operation was investigated.
- The tests were performed at 673 K and 723 K for various NaOH–KOH –LiOH mixtures.
- The cell was fueled with graphite rod and biochar.
- The best results were achieved for biochar and 50–50 mol% NaOH–KOH electrolyte.

GRAPHICAL ABSTRACT

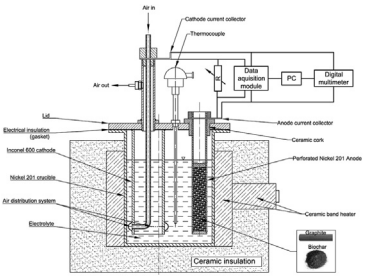

ARTICLE INFO

Article history:
Received 11 January 2013
Received in revised form
26 March 2013
Accepted 27 March 2013
Available online 8 April 2013

Keywords:
Direct carbon fuel cell
Biochar
Graphite
Molten hydroxide electrolyte

ABSTRACT

This paper describes the performance of a direct carbon fuel cell. Particular attention was made to investigate the effects of the composition and temperature of the electrolyte on cell operation and parameters. Various binary and ternary molten alkali hydroxides have been used as electrolytes. The performance of the fuel cell was investigated at various temperatures for four compositions of the electrolytes. Graphite rod and biochar (apple tree chips carbonized at 873 K) were used as fuels.

The experiments indicated that the composition of the electrolyte and temperature significantly affected the performance of the fuel cell. The best results were obtained for the fuel cell operated with biochar fuel and NaOH–KOH electrolyte (50–50 mol%) at 673 K.

1. Introduction

Over the past several decades fuel cell technologies have been treated as promising candidates for various utility applications. Today fuel cells are still considered an environmentally friendly and highly efficient electricity generating systems and extensive research has been conducted worldwide to improve this technology [1].

The direct carbon fuel cell (DCFC) is a unique type of fuel cell able to convert efficiently the chemical energy of solid carbonaceous fuels directly into electricity without the combustion of the fuels. The theoretical maximum efficiency of carbon conversion in the DCFC is 100% [2] but practical efficiencies have been demonstrated at roughly 80% [3]. This type of fuel cells has been under investigation for several years [2–4] since the technology is relatively simple compared to other fuel cell technologies and requires no expensive preparation of any gaseous fuel, and it is as well able to accept all carbonaceous substances as potential fuels. To run the DCFC and to generate electrical power one only needs to immerse

* Corresponding author. Tel.: +48 34 325 7334x18; fax: +48 34 325 7334x25.
E-mail addresses: rafalk@is.pcz.czest.pl, akacprzak@is.pcz.czest.pl (A. Kacprzak).

0378-7753/$ – see front matter © 2013 Elsevier B.V. All rights reserved.
http://dx.doi.org/10.1016/j.jpowsour.2013.03.159

solid carbon based material (i.e. granulate, rod, pellet, etc.) without any pretreatment at the anode and electrochemically oxidize it at high temperature according to Eq. (1). The standard potential for Eq. (1) is 1.02 V [2].

$$C + O_2 = CO_2 \quad (1)$$

There are three basic types of DCFCs. They generally differ with electrolyte types that can be molten carbonates, YSZ-based solid electrolytes, or molten hydroxides. The use of various types of electrolytes creates differences in electrochemical processes that occur at the electrodes and thus results in the potential difference between the electrodes. Regardless of the electrolyte, however, the product of the oxidation reactions is pure carbon dioxide.

Mixed molten carbonates, such as Na_2CO_3, Li_2CO_3, and K_2CO_3 are widely used as electrolytes, mainly due to their long-term stability in the presence of CO_2, as well as their high ionic conductivity and catalytic properties. However the disadvantages of such carbonate mixtures are high melting temperature (1023–1123 K) and chemical aggressiveness that can create intensive corrosion of the construction materials. An additional problem for this type of fuel cells, is the formation of CO that occurs via the Boudouard reaction at the anode side (Eq. (2)):

$$C_{(s)} + CO_{2(g)} = 2CO_{(g)} \quad (2)$$

The DCFC with solid electrolyte is usually a tubular or planar solid oxide fuel cell (SOFC), and yttria-stabilized zirconia (containing 8–10 mol% Y_2O_3) is the most commonly used electrolyte material. However, in order to ensure proper ionic conductivity of the solid electrolyte the cell has to be operated at high temperatures (above1073 K) that favor the formation of CO following Eq. (2) and causes the degradation of the cell construction materials, particularly the catalytic elements of the anode and the cathode.

By contrast, the use of electrolytes composed of molten hydroxides in the DCFC offers a number of advantages, such as high ionic conductivity and high electrochemical activity of the carbon. Accordingly, DCFC may be operated at lower temperatures (roughly 673–873 K) and thus cheaper materials may be used to manufacture the cell. The DCFC with molten hydroxides still suffers, however, from the formation of carbonates in the melt since the carbonates are formed via the reactions between the product CO_2 and the hydroxide ions in the melt.

As only a limited number of papers have been published on the operation of DCFCs with hydroxide electrolytes [5–10], there is still need for much research to be done to determine the effectiveness of the cell, the intention of this paper is provide some information on the performance of a model DCFC. Accordingly this paper describes the effects of the composition and temperature of molten hydroxide electrolytes of various different binary and ternary NaOH, KOH, and LiOH mixtures on the operation of the direct carbon fuel cell.

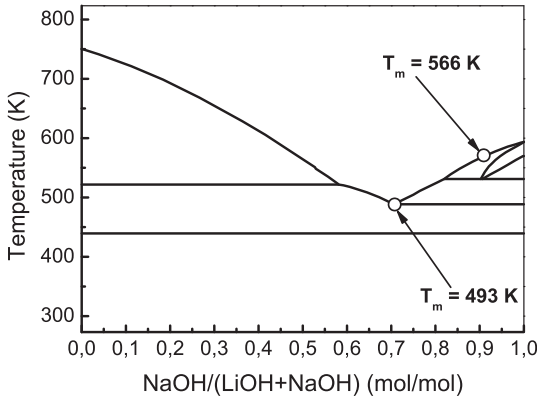

Fig. 1. Phase diagram for the NaOH–LiOH binary system [11].

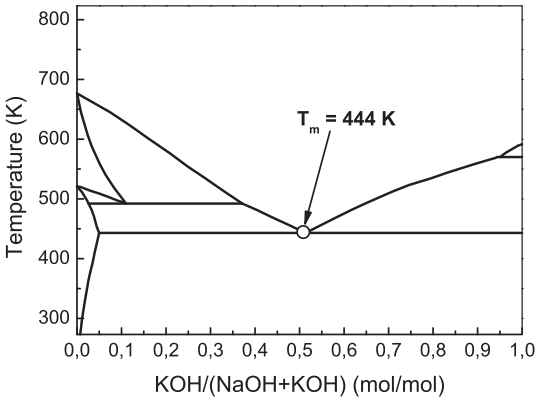

Fig. 2. Phase diagram for the NaOH–KOH binary system [11].

Table 1
Melting temperatures of some selected hydroxide mixtures.

Composition [mol%]	NaOH–LiOH (90–10)	NaOH–LiOH (70–30)	NaOH–KOH (50–50)
Melting temperature [K]	566	493	444

2. Experimental

2.1. Electrolytes and fuels

Three binary mixtures of alkaline earth metal hydroxides NaOH, KOH, LiOH (supplied by POCH and STANLAB corps.) were selected for the investigations. The compositions of the electrolyte mixtures for the DCFC were selected based on phase diagrams as shown in Figs. 1 and 2 and the data given in Table 1.

All the selected eutectic mixtures of the hydroxides are characterized by much lower melting temperatures compared to pure hydroxides (NaOH – 596 K, KOH – 679 K, LiOH – 746 K).

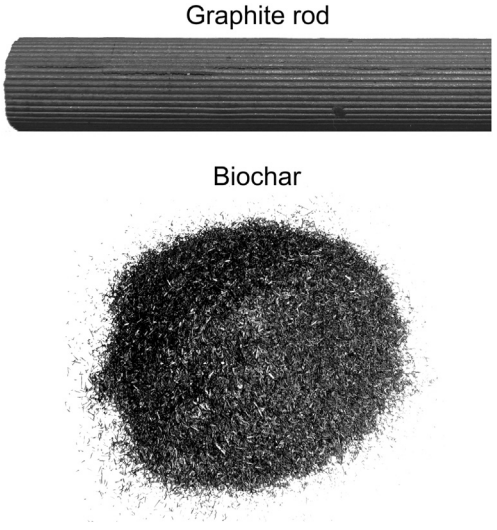

Fig. 3. Examples of solid fuel sample.

Table 2
The main parameters of the fuels (all values are given for a "dry" state).

Fuel type	Volatile matter (wt%)	Ash (wt%)	Fixed carbon (wt%)	Higher heating value [MJ kg^{-1}]	Elemental composition [wt%]				
					C	H	N	S	O^{diff}
Graphite rod	1.3	1.7	97.0	32.3	97.3	0.25	0.45	0.0	0.3
Biochar	16.1	11.6	72.3	29.6	80.3	2.8	1.9	0.0	3.4

The tests with the DCFC were performed at two temperatures: 673 K and 723 K. The air supplied to the fuel cell was fed from a compressor at a flow rate of 0.5 dm^3 min^{-1}.

The fuels used for the investigation were graphite electrode (reference fuel) and biochar. The biochar was derived from the carbonization of apple tree chips (particle size <0.5 mm) at 873 K for 30 min. The details of the biomass carbonization technology have been described elsewhere [12–14].

The two selected fuels are shown in Fig. 3. Both were analyzed according to Polish standards for those type of fuels. The automatic isoperibol calorimeter (IKA C2000 Basic) was used to determine the higher heating values (HHV) of the samples. The ultimate analyses were determined with the use of Leco TruSpec CHNS analyzer. The results of the analyses are summarized in Table 2.

2.2. DCFC test setup

The experiments were conducted in a laboratory-scale DCFC test cell shown schematically in Fig. 4.

The body of the cell setup was manufactured from nickel and nickel alloys. The anode and cathode chambers were separated in order to prevent any mixing at the gases (CO_2 above the anode and excess air above the cathode). The main cell container (83 mm i.d. and roughly 147 mm high) was manufactured from Nickel® 201. The anode was made from Nickel® 201, while the cathode was Ni-based Inconel® alloy 600.

The anode and cathode were specially designed 'pipe-type' constructions with outside diameters of 19.1 mm and 42 mm, respectively. However, to make things simpler, in the case of the tests with graphite fuel, the anode construction was removed and replaced by a graphite rod.

The components of the prototype, particularly the anode and cathode pipes, were subjected to simultaneous oxidation and lithiation process, since the doping of cation-defective p-type nickel oxides by lower valence (Li^+) cations makes the NiO highly conductive. Such highly conductive materials are crucial to ensure good performance of the electrodes [15]. The lithiation of the NiO cathode was conducted by simultaneous oxidation and lithium-doping of the Ni-base cathode material. The nickel was oxidized to NiO while simultaneously the lithium ions were incorporated into the NiO matrix at the surface zone. Source of Li^+ ions was lithium hydroxide monohydrate ($LiOH \cdot H_2O$, melting temperature 743 K). In order to accelerate the oxidation of nickel to NiO immediately after the lithium hydroxide became molten the air was fed into the system at a flow rate of 0.2 dm^3 min^{-1}. The process was carried out at 873 K for 24 h. The anode and cathode materials were then slowly cooled to ambient temperature and washed several times in distilled water and HCl solution to remove and neutralize any residual lithium hydroxide. The cell components were then dried in an oven for 2 h.

The temperature of the electrolyte was determined by a K-type thermocouple (NiCr–NiAl) and was maintained at the desired

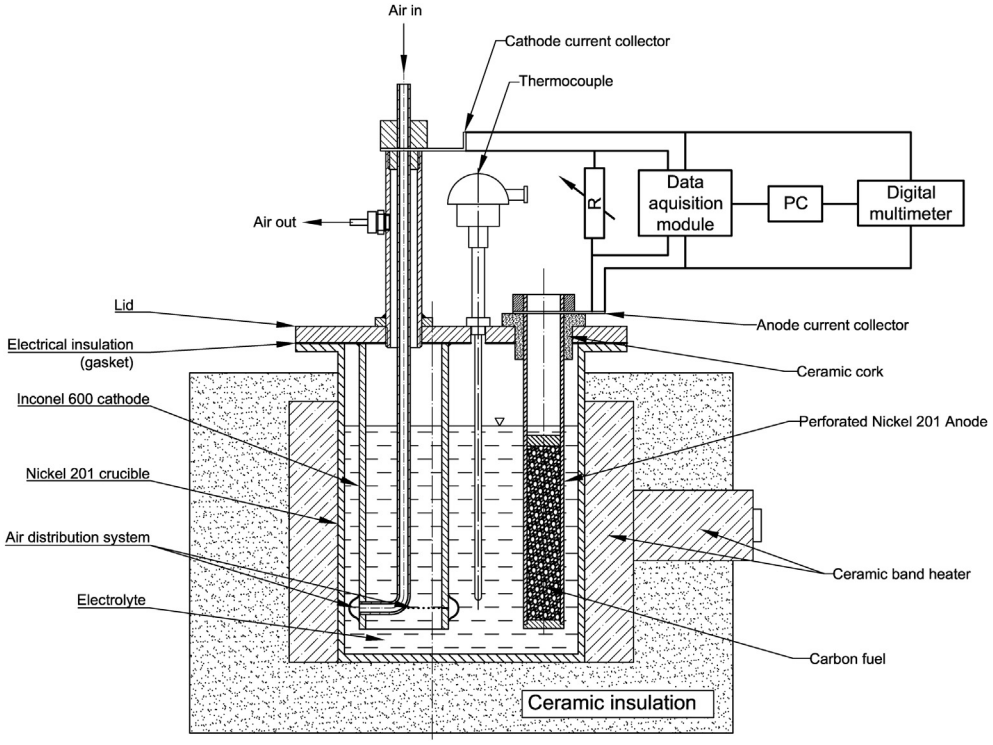

Fig. 4. The outline of the experimental DCFC setup.

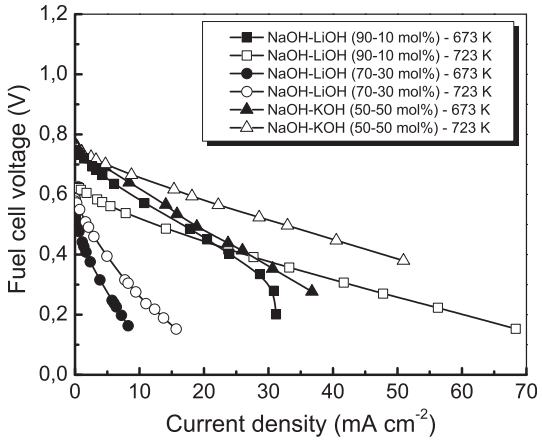

Fig. 5. Cell voltage vs. current density for the DCFC (fuel: graphite, air flow rate: 0.5 dm^3 min^{-1}).

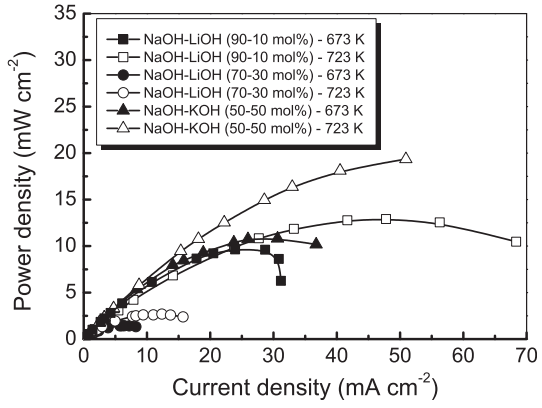

Fig. 6. Power density vs. current density for the DCFC (fuel: graphite, air flow rate: 0.5 dm^3 min^{-1}).

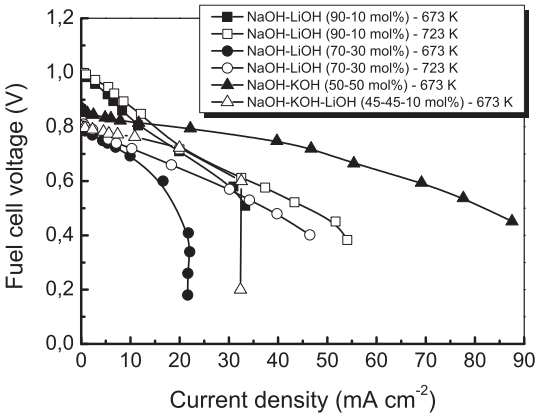

Fig. 7. Cell voltage vs. current density for the DCFC (fuel: biochar, air flow rate: 0.5 dm^3 min^{-1}).

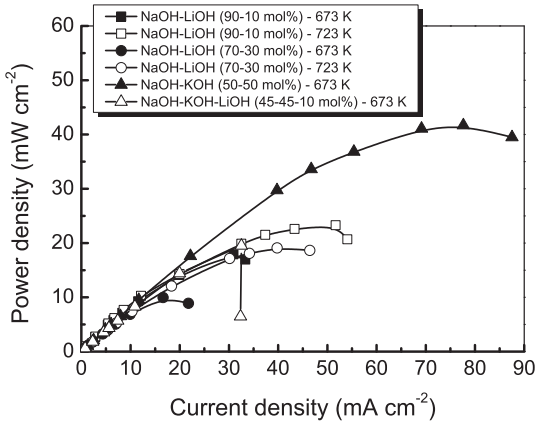

Fig. 8. Power density vs. current density for the DCFC (fuel: biochar, air flow rate: 0.5 dm^3 min^{-1}).

value by an electronic temperature controller. The data acquisition module Advantech USB-4711A was used to measure the cell voltage and the loss of the voltage on an external resistor. The module was connected to a personal computer (PC) where the data were displayed and stored. The Tektronix DMM4040 Digital Multimeter was applied to measure the open circuit voltage of the fuel cell. In order to determine the cell current at various loads an external resistance setup MDR-93/2-52 was connected to the cell circuit thus providing the possibility to adjust the electrical resistance of the external circuit over a wide range (0.1–10,000 Ω). The amount of air fed into the cell was controlled by a mass flow controller (Brooks 4850). The gas flow rate could be adjusted from 0.1 dm^3 min^{-1} to 2.0 dm^3 min^{-1}.

In order to attenuate short-term surge suppression and eliminate the effects of power grid interferences on the recorded data the emergency standby backup power device, PowerCom UPS BNT-1500AP with a noise filter EMI/RFI, was used during the experiments. The tool also acted as an 'emergency power supply device' for the data recording system in case of any power failure.

2.3. Experimental procedure

At the beginning of each test the appropriate mole fractions of hydroxides were weighted and mixed. The mixture was then put into the main cell container and heated to the desired temperature. After the temperature level was reached and the electrolyte became completely molten the cathode and the anode were slowly immersed into the electrolyte. The cell data (current intensity, voltage, temperature, etc.) were then continuously recorded. The voltage–current and power–current characteristics of the cell were determined for the data taken after 4 h of continuous cell operation without an external load.

Table 3
Summary of the operation parameters for DCFC (various electrolytes, fuel: graphite rod).

Electrolyte composition [mol%]	Temperature [K]	Electromotive force [V]	Maximum power density [mW cm^{-2}]	Current density at 0.5 V [mA cm^{-2}]
NaOH–LiOH (90–10)	673	0.7452 ± 0.0002	9.6	16.6
	723	0.6791 ± 0.0019	12.9	12.5
NaOH–LiOH (70–30)	673	0.5298 ± 0.0005	1.5	0.3
	723	0.5859 ± 0.0008	2.7	1.9
NaOH–KOH (50–50)	673	0.7653 ± 0.0004	10.8	18.4
	723	0.7693 ± 0.0011	19.4	32.4

Table 4
Summary of the operation parameters for DCFC (various electrolytes, fuel: biochar).

Electrolyte composition [mol%]	Temperature [K]	Electromotive force [V]	Maximum power density [mW cm^{-2}]	Current density at 0.5 V [mA cm^{-2}]
NaOH–LiOH (90–10)	673	0.9985 ± 0.0003	17.9	33.3
	723	1.0008 ± 0.0005	22.4	44.6
NaOH–LiOH (70–30)	673	0.8048 ± 0.0039	10.0	19.3
	723	0.8434 ± 0.0036	19.1	37.9
NaOH–KOH (50–50)	673	0.8726 ± 0.0024	41.7	81.9
NaOH–KOH–LiOH (45–45–10)	673	0.8104 ± 0.0018	19.5	32.4

After the test was finished the heating was turned off and the cell was 'shutdown'. The setup was then cooled to room temperature and then all its parts were placed in a special plastic container filled with roughly 25 L of deionized water. All the elements were kept there for 3 h in order to remove any solidified electrolyte. A mechanical stirrer was used to improve the dissolution of the electrolyte. The water–electrolyte mixture was then removed and a new batch of 25 L of deionized water was put into the container and the whole procedure was repeated. Afterward, all the cell elements were removed from the container and cleaned with a soft sponge, and finally again rinsed with deionized water. All the elements were then dried for 2 h in an oven.

3. Results and discussion

3.1. Experiments with graphite rod

The polarization and power characteristics of the cell operated with various electrolytes (NaOH–LiOH and NaOH–KOH mixtures) and at various temperatures are shown in Figs. 5 and 6, respectively. The main operation parameters of fuel cell are summarized in Table 3.

The results in Figs. 5 and 6 and Table 3 indicated that the best electrochemical activity (highest OCV and highest power and current densities at 723 K) was achieved for NaOH–KOH (50–50 mol%) electrolyte while the worst results (<3 mW cm^{-2}) were determined for NaOH–LiOH (70–30 mol%). It could be seen that the increase of the temperature of the electrolyte brought about the increases of the OCV and power density. The increase of the temperature from 673 K to 723 K significantly increased the maximum power density (up to almost 20 mW cm^{-2}), probably due to the increase of the rates of the electrochemical reactions. Furthermore, the increase of the temperature improved the ionic conductivity of the electrolyte and this could also have an impact on the operation of the fuel cell.

Although, as it is shown in Table 3, the highest power density and current density were measured for the DCFC operated with NaOH–KOH (50–50 mol%) electrolyte, the addition of some LiOH is recommended from a practical point of view, even if the addition of LiOH to the electrolyte mixture worsens the performance of the fuel cell (cf. Figs. 5 and 6). This is because the addition of Li^+ ions improves the electrical conductivity of the NiO matrix (cf. Section 2.2 of this paper and e.g. Ref. [15]) and furthermore decreases the melting temperature of NaOH–KOH mixture (cf. Figs. 1 and 2) thus minimizing the amount of heat supplied to the DCFC and required to maintain the electrolyte in a molten state.

3.2. Experiments with biochar

The fuel cell voltage and power density curves as functions of current density for various electrolytes and biochar fuel are shown in Figs. 7 and 8. The main cell parameters are summarized in Table 4.

As shown in Figs. 7 and 8 and in Table 4 the best performance of the cell (i.e., current and power density) was obtained for the electrolyte composed of NaOH–KOH (50–50 mol%) at 673 K. Similar to the results for graphite, the increase of temperature caused the increase of the cell operating parameters (power densities have increased by 25% and 91%, current densities have increased by 34% and 96% depending on the electrolyte composition). The results also indicated that the biochar was more reactive than graphite, probably due to its properties (structure, degree of graphitization, particle size, pore size distribution and surface area). The advantages of biochar compared to graphite fuel were also reported by Ref. [4].

As already discussed before the addition of some Li^+ ions to the electrolyte was welcomed even if it worsened the cell performance (cf. Figs. 5 and 6 and Table 3 for the case of graphite fuel). The authors decided to check if similar situation could happened for biochar fueled DCFC in the case 10 mol% of lithium hydroxide would be added to 'the best' electrolyte (NaOH–KOH, cf. Tables 3 and 4).

The corresponding data for NaOH–KOH–LiOH electrolyte (45–45–10 mol%, respectively) indicated that the presence of lithium hydroxide changed the properties of the electrolyte and resulted in the degradation of the fuel cell performance. As shown in Figs. 7 and 8 and in Table 4 the electromotive force, as well as the power- and current densities, were significantly lower than for the previous test when no LiOH was added.

Although, the best results were obtained for electrolytes without the addition of lithium hydroxide the lack of Li^+ ions did not allow the *in-situ* lithiation process to happen. This might in a long-term operation bring about the decrease of the electrical conductivity of the passive layer that was formed on the electrode surface. Consequently, the process might result in a fuel cell emergency shutdown. Since there is still much work to do to explain in detail the processes running on the surface of carbonaceous materials in molten hydroxide electrolytes the authors plan to conduct a long term tests in the near future to investigate whether the presence of Li^+ ions is really essential for stable and continuous operation of the DCFC.

4. Conclusions

From the experimental results presented and briefly discussed in the present paper the following conclusions can be formulated:

1. Four compositions of molten hydroxide electrolytes were tested to investigate the optimum electrolyte composition for the DCFC fueled with graphite rod and biochar.
2. During the experiments the cell power densities ranged from 1.5 mW cm^{-2} to 41.7 mW cm^{-2} and the current densities from 0.3 mA cm^{-2} to 81.9 mA cm^{-2}. The highest maximum power density and current density were achieved for biochar fueled DCFC with NaOH–KOH (50–50 mol%) electrolyte.
3. The increase of the molar fraction of LiOH in the molten electrolyte mixture worsened the performance of the fuel cell (lower OCV and lower power and current densities).
4. Biochar fuel was much more reactive than graphite rod. The differences were probably associated with the structure of the carbon matrix, as well as the degree of crystallinity of the carbon.

5. From all the investigated hydroxides the best results were achieved for 1:1 mixture (molar ratio) of NaOH and KOH, and 9:1 mixture of NaOH and LiOH. The first type of electrolyte allows to operate the DCFC at lower temperature.

Acknowledgment

This work has been supported by the Polish Ministry of Education and Science under grant no. N N513 396 736.

One of the authors (A. Kacprzak) is also indebted for the financial support to the DoktoRIS – Scholarship Program for Innovative Silesia, co-financed by the European Union within the framework of the European Social Fund.

References

[1] D. Oertel, T. Fleischer, A. Soria (Eds.), Fuel Cells, Impact and Consequences of Fuel Cells Technology on Sustainable Development, An ESTO Project Report Prepared for Prospective Technology Studies Joint Research Centre by Institut für Technikfolgenabschätzung und Systemanalyse (ITAS) (March 2003).
[2] D. Cao, Y. Sun, G. Wang, Journal of Power Sources 167 (2007) 250–257.
[3] J.F. Cooper, in: S. Basu (Ed.), Recent Trends in Fuel Cell Science and Technology, Springer and Anamaya, 2007, pp. 248–266. (Chapter 10).
[4] S. Giddey, S.P.S. Badwal, A. Kulkarni, C. Munnings, Progress in Energy and Combustion Science 38 (2012) 360–399.
[5] S. Zecevic, E.M. Patton, P. Parhami, Carbon 42 (2004) 1983–1993.
[6] S. Zecevic, E.M. Patton, P. Parhami, Chemical Engineering Communications 192 (2005) 1655–1670.
[7] G.A. Hackett, J.W. Zondlo, R. Svensson, Journal of Power Sources 168 (2007) 111–118.
[8] A. Kacprzak, R. Kobyłecki, Z. Bis, Środowisko i Rozwój 22 (2/2010) 87–100 (in Polish).
[9] A. Kacprzak, R. Kobyłecki, Z. Bis, Archives of Thermodynamics 32 (3/2011) 37–47.
[10] A. Kacprzak, M. Kratofil, R. Kobyłecki, Z. Bis, Characteristics of operation of direct carbon fuel cell, in: Proc. IX Conf. RDPE 2011, Research and Development in Power Engineering, 2009, (in Polish).
[11] FTsalt–FACT Salt Phase Diagrams, Centre for Research in Computational Thermochemistry (CRCT), Facility for the Analysis of Chemical Thermodynamics (FACT), 2012. http://www.crct.polymtl.ca/fact.
[12] R. Kobyłecki, Z. Bis, The carbonization of biomass for renewable energy and carbon sink, in: Proc. of the 3rd Int. Conf. on Contemporary Problems of Thermal Engineering, CPOTE 2012, Gliwice, Poland, September 18–20, 2012, pp. 185–186, ISBN: 978-83-61506-13-3.
[13] R. Kobyłecki, Z. Bis, Archiwum Spalania. ISSN: 1641-8549, vol. 6 (1–4) (2006) 114–119 (in Polish).
[14] R. Kobyłecki, J. Tchórz, Z. Bis, Densification of biomass energy for large scale Co-combustion, in: Proc. of the 9th Int. Conf. on Circulating Fluidized Beds (CFB-9) in Conjunction with 4th Int. VGB Workshop, Hamburg, Germany, May 13–16, 2008, pp. 839–843, ISBN: 978-3-930400-57-7.
[15] P. Kalyani, N. Kalaiselvi, Science and Technology of Advanced Materials 6 (2005) 689–703.